Stabilization of the spinel structure in Li$_{1+\delta}$Mn$_{2-\delta}$O$_4$ obtained by sol–gel method

R. Dziembaj[a,b,*], M. Molenda[a]

[a]*Faculty of Chemistry, Jagiellonian University, Ingardena 3, 30-060 Cracow, Poland*
[b]*Regional Laboratory of Physicochemical Analyses and Structure Researches,*
Ingardena 3, 30-060 Cracow, Poland

Abstract

The lithium–manganese-oxide spinels with different δ values (from 0 to 0.20) were obtained by sol–gel method and studied using XRD, TGA/SDTA, DSC and electrical conductivity measurements. Transformation of the initial gels to spinel structure results in a strong exothermic effect in SDTA measurement. It was shown that well-crystallized spinel structures with cationic defects Li$_{1-x}$Mn$_{2-2x}$O$_4$, are formed after calcination at 300 °C (low-temperature spinel). Evolution of oxygen during thermal treatment of the low-temperature spinel was controlled by TGA/SDTA methods. Three stages of this transformation were distinguished and one of them was irreversible. The electrical conductivity of the spinels correlates with thermal properties and phase changes in the spinels.
© 2003 Elsevier Science B.V. All rights reserved.

Keywords: Li-ion batteries; LiMn$_2$O$_4$ properties; Phase transition

1. Introduction

Li$_{1+\delta}$Mn$_{2-\delta}$O$_4$, "the δ-spinel", is a cathode material for 4 V rechargeable lithium batteries which perhaps in the future will be used instead of the toxic LiCoO$_2$ cathodes [1–3]. The δ-spinels are usually obtained by high-temperature calcinations of oxide, carbonate and/or hydroxide precursor mixtures [4,5]. The δ excess of lithium protects the Li–Mn-oxide spinels against the first order phase transition from cubic $Fd\bar{3}m$ to orthorhombic Fddd structure at about room temperature, but decreases the capacity of the electrode material due to substitution of Mn^{3+} ions in octahedral sites. This transition related to Jahn–Teller distortion causes losses in the capacity of cathode material and electrical conductivity [6,7].

An alternative method of Li–Mn spinel formation is the sol–gel method followed by low-temperature calcination [8,9]. It was shown that even 300 °C is enough to get material showing the XRD pattern characteristic for the spinel structure [9]. Such a material does not show the phase transition at room temperature though its electrical properties are worse than those of the high-temperature calcined

materials [10]. The materials obtained by "soft chemistry" methods show better performance due to smaller crystallites and larger surface area [8].

The present paper concerns thermal decomposition of the Li–Mn gels, their transformation into spinel structure and changes in electrical conductivity and thermal stability of the materials obtained by sol–gel method.

2. Experimental

The appropriate amounts of precursors LiNO$_3$ (Aldrich, SigmaUltra, 99.99%) and Mn(CH$_3$COO)$_2$·4H$_2$O (Aldrich, 99.99%), were dissolved in de-ionized water, transformed into gel by slowly adding concentrated ammonia solution, and then dried. All these operations were done under argon atmosphere [9]. The resulting materials were calcined at temperatures between 300 and 800 °C for 24 h and subsequently quenched.

DSC experiments were performed on a Mettler-Toledo 821^e in 40 µl aluminum crucibles under flow of argon. The TGA/SDTA experiments were performed on a Mettler-Toledo 851^e in platinum crucibles under flowing air.

The XRD powder diffraction patterns were recorded during heating in situ with a Philips X'Pert using Cu Kα radiation. The data were analysed by the Rietveld method using JCPDS standards [11].
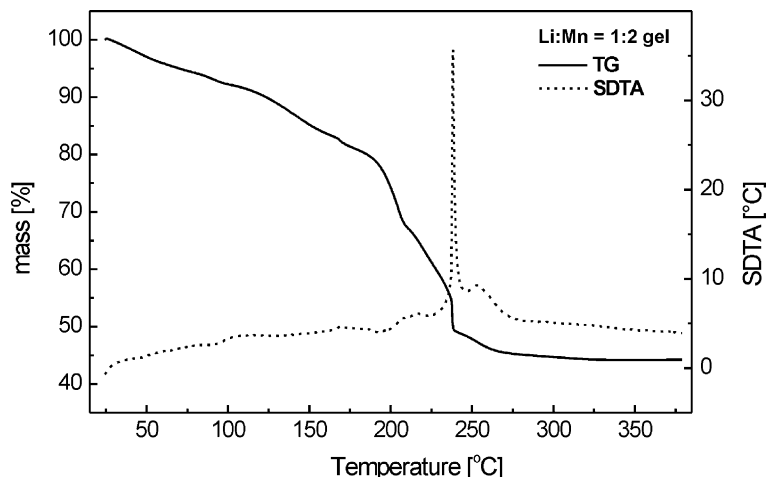
Fig. 1. TGA/SDTA of thermal decomposition of the Li:Mn = 1:2 gel.

Electrical conductivity was measured using a four probe method within the range -40 to $+35\,^\circ\mathrm{C}$. To improve the electric contact, a silver paste with acrylic resin was used.

3. Results and discussion

The thermal decomposition of the "stoichiometric" (Li:Mn = 1:2) gel is presented in Fig. 1. Thermal decomposition of the Li–Mn gels starts just above the room temperature but accelerates above $180\,^\circ\mathrm{C}$. There is a sudden mass loss accompanied by strong exothermic effects. They are related to acetate and Mn^{2+}-ion oxidation and the Li–Mn spinel formation. The samples calcined up to $300\,^\circ\mathrm{C}$ and cooled to room temperature show the XRD pattern characteristic for Li–Mn spinels [9].

The result of further heating of the Li:Mn = 1:2 sample are presented in Fig. 2. The evolution of oxygen begins above $350\,^\circ\mathrm{C}$ with acceleration above $820\,^\circ\mathrm{C}$. Very fast decomposition of sample takes place above $920\,^\circ\mathrm{C}$. During cooling,

the samples incorporate oxygen up to the concentration fit for the stoichiometric $LiMn_2O_4$ spinel. The next heatings of the sample show no decomposition effects within the temperature range RT–$820\,^\circ\mathrm{C}$. The thermogrammes overlap each other in both directions.

The following reactions describe thermal decomposition of the Li–Mn spinels:

I. $Li_{1-x}Mn_{2-2x}O_4 \rightarrow (1-x)LiMn_2O_4 + 2xO_2 \uparrow$ (RT – $820\,^\circ\mathrm{C}$)

II. $LiMn_2O_4 \leftrightarrow LiMn_2O_{4-y} + \frac{1}{2}yO_2 \uparrow$ (820–$920\,^\circ\mathrm{C}$)

III. $3LiMn_2O_{4-y} \leftrightarrow 3LiMnO_2 + Mn_3O_4 + (1 - \frac{3}{2}y)O_2 \uparrow$ (above $920\,^\circ\mathrm{C}$)

The lattice parameter a of the Li–Mn spinel (measured in situ) increases with temperature (Fig. 2). The acceleration of the oxygen evolution above $400\,^\circ\mathrm{C}$ is accompanied by a faster increase in the lattice parameter. The coefficient of thermal expansion for the Mn^{4+}-rich spinel estimated from the obtained results is about one order smaller than that for the Li–Mn spinel with a ratio of $Mn^{3+}:Mn^{4+}$ close to 1.

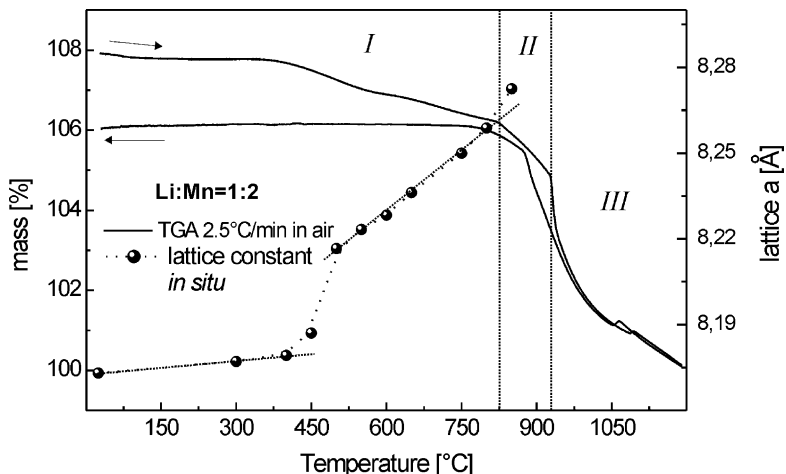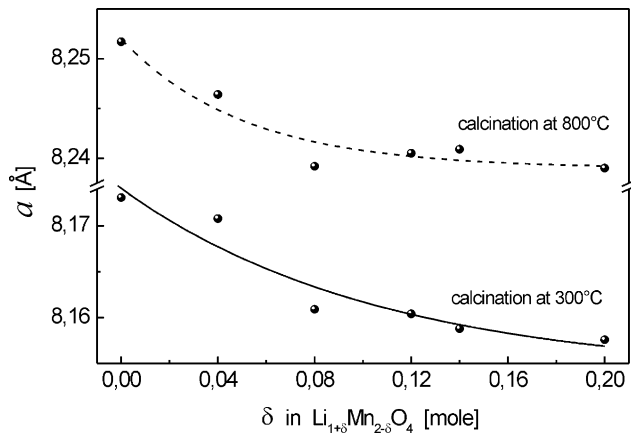Fig. 2. TGA of S300 sample (Li:Mn = 1:2) vs. lattice constant a in situ.

Fig. 3. Dependence of lattice constant a of $Li_{1+\delta}Mn_{2-\delta}O_4$ spinels calcined at 300 and 800 °C on lithium excess.

The step in the lattice parameter is due to reaction I which is related to ordering of the spinel structure connected with disappearance of the cation vacancies. This change in the structure is irreversible.

The appearance of the oxygen deficient material described by reaction II was previously proposed by Tarascon et al. [12]. This evolution of oxygen causes reduction of Mn^{4+} ions and in consequence formation of the tetragonal spinel phase ($Mn^{3+}:Mn^{4+} > 1$). The final composition of the tetragonal phase was determined to be $LiMn_2O_{3.86}$, very close to that proposed by Tarascon.

The δ-spinel samples, i.e. showing an excess of lithium ($0 \leq \delta \leq 0.20$), show similar changes in the lattice a parameter with increase of δ, independent of temperature of calcination (Fig. 3). The decrease in lattice parameter results from the decrease in concentration of Mn^{3+} ions (1δ Li^+ ions eliminate 3δ Mn^{3+} ions), which are significally larger than Mn^{4+} ions. Calcination at 800 °C provides materials with better crystallinity and larger lattice constants due to a better ordered spinel structure.

The results of the DSC measurements are presented in Fig. 4. The stoichiometric spinel (Li:Mn = 1:2) calcined within 300–600 °C does not show the low-temperature phase change related to the Jahn–Teller distortion. With
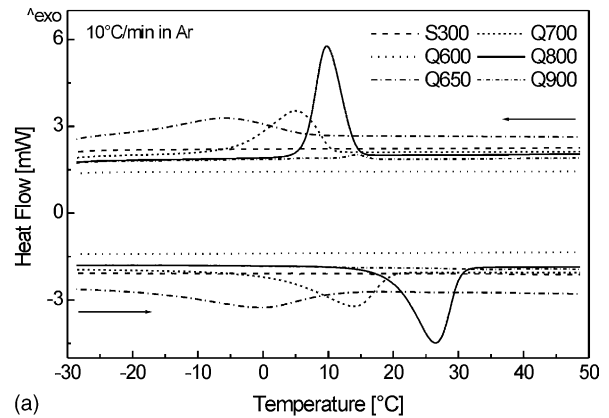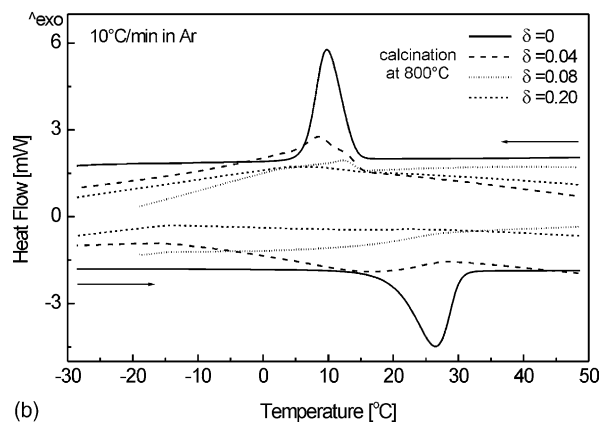
Fig. 4. DSC measurements of (a) spinel Li:Mn = 1:2 calcined within temperatures 300–900 °C, (b) $Li_{1+\delta}Mn_{2-\delta}O_4$; $\delta = 0.0$, 0.04, 0.08 and 0.20 calcined at 800 °C.

an increase in the calcination temperature, the gradually increased effects of this phase change appear (Fig. 4a). A similar influence is observed due to introduction of excess lithium ($\delta > 0.04$). The results are presented in Fig. 4b.

Analysis of the Mn^{3+} situation in the spinel structure shows an interesting rule. If the atomic ratio of Li^+ placed in tetrahedral sites and Mn^{3+} is limited to values between 1.00 and 1.14, the low-temperature phase change appears. This value can be controlled by temperature of calcination, as well as by lithium excess (Table 1).

Table 1
Distribution of cations sites in spinel structure on phase transition

Sample	Composition			Li^+_{8a}	Mn^{3+}_{16d}	$Li^+_{8a}: Mn^{3+}_{16d}$	Phase transition at about 290 K
	Li	Mn	O				
S300	0.96	1.92	4	0.96	0.64	1.50	No
Q600	0.98	1.96	4	0.98	0.82	1.20	No
Q650	0.985	1.97	4	0.985	0.87	1.13	Yes
Q700	0.99	1.98	4	0.99	0.91	1.09	Yes
Q800	1	2	4	1.00	1.00	1.00	Yes
Q900	1	2	3.9	1.00	1.20	0.83	No
$\delta = 0.04$	1.04	1.96	4	1.00	0.88	1.14	Yes
$\delta = 0.08$	1.08	1.92	4	1.00	0.76	1.32	No
$\delta = 0.20$	1.20	1.80	4	1.00	0.40	2.50	No

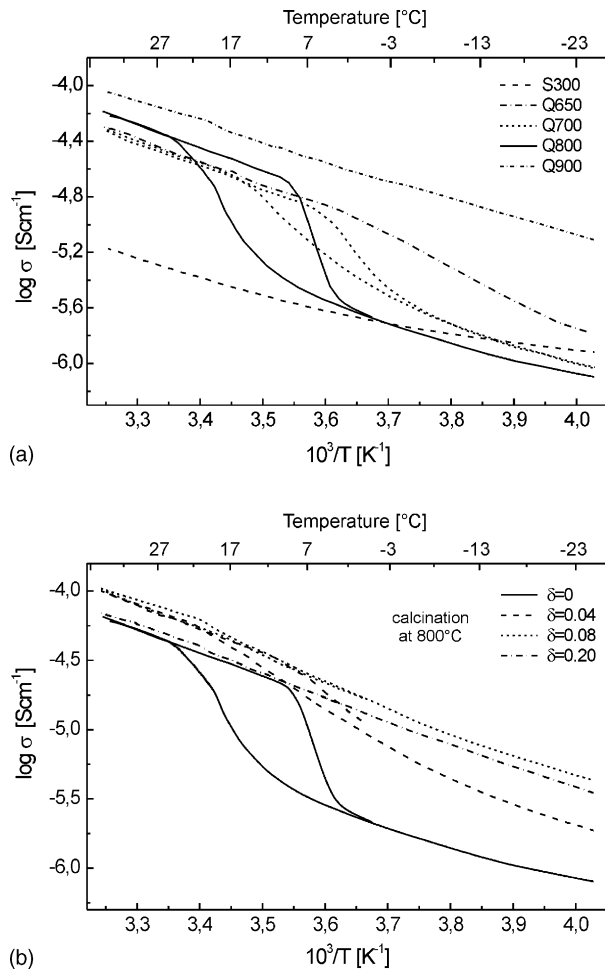8a and 16d index describe the different sites of ions in Wyckoff notation, tetrahedral and octahedral, respectively.

Fig. 5. Electrical conductivity of (a) spinel Li:Mn = 1:2 calcined within temperatures 300–900 °C, (b) $Li_{1+\delta}Mn_{2-\delta}O_4$; $\delta = 0.0$, 0.04, 0.08 and 0.20 calcined at 800 °C.

The results of electrical conductivity measurements correlate well with results of the DSC measurements (Fig. 5). Calcination temperature and Li content can be varied to suppress features observed near room temperature on both curves. The hysteresis loop in the conductivity measurements disappears under similar conditions as the peaks in the DSC experiments. There are stepwise changes in the curves for the samples in which we observe phase transitions—the orthorhombic phase is much more resistive. The activated character of the electrical conductivity suggests a small polaron conduction mechanism. The electrical conductivity is improved with increase of the calcination temperature. It results from the better structural ordering rather than from the higher concentration of effective carriers, given by the formula $[Mn^{3+}][Mn^{4+}]$.

It may be concluded that recommended temperatures of calcination for sol–gel obtained spinels should be close to 600 °C. Similarly, the best electrical properties of the $Li_{1+\delta}Mn_{2-\delta}O_4$ cathode material obtained by the sol–gel methods are expected for a small lithium excess ($\delta \leq 0.04$).

Acknowledgements

References

[1] J.M. Tarascon, E. Wang, F.K. Shokoohi, W.R. Mc Kinnon, S. Colson, J. Electrochem. Soc. 138 (1991) 2859.
[2] M.M. Thackeray, M.F. Mansuetto, D.W. Dees, D.R. Vissers, Mater. Res. Bull. 31 (1995) 133.
[3] C. Masquelier, M. Tabuchi, K. Ado, R. Kanno, Y. Kobayashi, Y. Maki, O. Nakamura, J.B. Goodenough, J. Solid State Chem. 123 (1996) 255.
[4] Y. Gao, J.R. Dahn, J. Electrochem. Soc. 143 (1996) 1783.
[5] T. Takada, H. Hayakawa, H. Enoki, E. Akiba, H. Slegr, I. Davidson, J. Murray, J. Power Sources 81–82 (1999) 505.
[6] G. Rousse, C. Masquelier, J. Rodriguez-Carvajal, M. Hervieu, Electrochem. Solid-State Lett. 2 (1999) 6.
[7] A. Yamada, M. Tanaka, K. Tanaka, K. Sekai, J. Power Sources 81–82 (1999) 73.
[8] L. Chen, X. Huang, E. Kelder, J. Schoonman, Solid State Ionics 76 (1995) 91.
[9] R. Dziembaj, M. Molenda, D. Majda, S. Walas, Solid State Ionics 157 (2003) 81.
[10] M. Molenda, R. Dziembaj, Phase transition disappearance in $Li_{1+\delta}Mn_{2-\delta}O_4$ depended on lithium excess, in: C. Julien, et al. (Eds.), New Trends in Intercalation Compounds for Energy Storage, NATO Science Series, Mathematics, Physics and Chemistry. Part II, vol. 61, Kluwer Academic Publishers, Dordrecht, 2002, p. 615.
[11] J. Rodriguez-Carvajal, G. Rousse, C. Masquelier, M. Hervieu, Phys. Rev. Lett. 81 (1998) 4660.
[12] J.M. Tarascon, W.R. McKinnon, F. Coowar, T.N. Bowmer, G. Amatucci, D. Guyomard, J. Electrochem. Soc. 141 (1994) 1421.